This is the author's version of an article that has been published in this journal. Changes were made to this version by the publisher prior to publication.
The final version of record is available at http://dx.doi.org/10.1109/TASC.2016.2521896

FERMILAB-CONF-15-439-TD
ACCEPTED

Longitudinal Gradient Dipole Magnet Prototype for APS at ANL

V.S. Kashikhin, M. Borland, G. Chlachidze, G. Decker, R. Dejus, J. DiMarco, C.L. Doose, T.J. Gardner, D.J. Harding, M.S. Jaski, J.S. Kerby, A.V. Makarov

***Abstract*— An upgrade of the Advanced Photon Source (APS) is being planned at Argonne National Laboratory (ANL). The main goal of the upgrade is to improve the storage ring performance based on more advanced optics. One of the key magnet system elements is bending dipole magnets having a field strength change along the electron beam path. A prototype of one such longitudinal gradient dipole magnet has been designed, built, and measured in a collaborative effort of ANL and Fermilab. This paper discusses various magnetic design options, the selected magnet design, and the fabrication technology. The prototype magnet has been measured by rotational coils, a stretched wire, and a Hall probe. Measurement results are discussed and compared with simulations.**

***Index Terms*—Accelerator, Photon Source, Dipole Magnet, Design, Fabrication, Magnetic Measurements.**

I. Introduction

ANL APS upgrade [1] is based on more advanced optics [2] for the existing accelerator. There are many synchrotron radiation sources in the world. The latest achievement explores in the magnet system lattice bending magnets with the longitudinal field gradient [3]. These magnets have a rapid field strength change along the electron beam path [1] – [3]. In the paper described the dipole magnet prototype which was designed, built, and tested by ANL-FNAL collaboration.

II. L-Bend Dipole Magnets Design

L-Bend magnets (see Fig. 1) generate the vertical dipole magnetic field to bend the electron beam. The main difference relatively conventional dipole magnets is that they have the field gradient along the beam path. Table 1 shows M1 and M2 magnets functional specifications. For the convenience of beam optics analysis each magnet has 5 sections with a different peak field (**B**), an effective length (**Leff**), and an integrated strength (**B×Leff**). The total magnet integrated strength defines the beam bending angle.

Manuscript received October 15, 2015. This work was supported in part by Fermi Research Alliance, LLC, under contract No. DE-AC02-07CH11359 with the U.S. Department of Energy. V.S. Kashikhin#, G. Chlachidze, J. DiMarco, T.J. Gardner, D.J. Harding, A.V. Makarov are with Fermi National Accelerator Laboratory, USA, M. Borland, G. Decker, R. Dejus, C.L. Doose, M.S. Jaski, J.S. Kerby are with Argonne National Laboratory, USA. (corr. author # (phone: 630-840-2899; fax: 630-840-6766; e-mail: kash@fnal.gov).

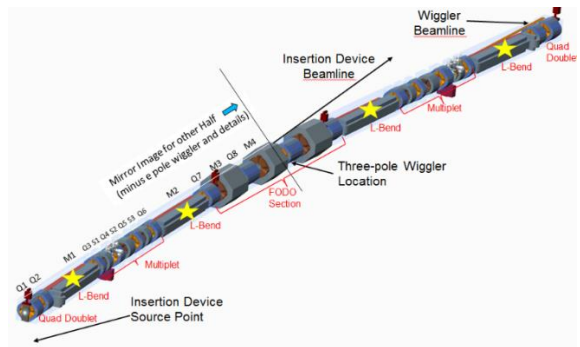

Fig. 1. The L-Bend magnets in one sector (highlighted with yellow stars).

One could see that for M1 magnet the peak field is about 5 times larger at the front magnet end than for the far magnet end. The M2 magnet has a shallower field profile along the beam path. All magnets will be powered from DC power supplies, should have the 20 mm minimum aperture with 0.1 % of the integrated field quality.

TABLE 1
Gradient Dipole Parameters

M1 Dipole			M2 Dipole		
B, T	**Leff, m**	**B×Leff, T-m**	**B, T**	**Leff, m**	**B×Leff, T-m**
0.634	0.187	0.11856	0.345	0.524	0.18078
0.341	0.216	0.07366	0.24	0.348	0.08352
0.226	0.606	0.13696	0.194	0.505	0.09797
0.138	0.794	0.10957	0.19	0.323	0.06137
0.131	0.364	0.04768	0.127	0.377	0.04787
Total	**2.167**	**0.48643**	**Total**	**2.077**	**0.47151**

There are several options to design this magnet type:

1. H-type or C-type magnet design.
2. Coils around poles or on the yoke backleg.
3. Five dipole magnet sections having the same air gap where the field gradient obtained by the separate coils ampere-turns variations.
4. The same as 3 but with the single coil having ampere-turns variations along Z-direction.
5. C-magnet with the single coil on the backleg of the yoke. The field gradient along Z-axis obtained by the magnet air gap variation.
6. The same as above but based on permanent magnets.

Operated by Fermi Research Alliance, LLC under Contract No. De-AC02-07CH11359 with the United States Department of Energy

Copyright (c) 2016 IEEE. Personal use is permitted. For any other purposes, permission must be obtained from the IEEE by emailing pubs-permissions@ieee.org.

This is the author's version of an article that has been published in this journal. Changes were made to this version by the publisher prior to publication.
The final version of record is available at http://dx.doi.org/10.1109/TASC.2016.2521896

For the APS storage ring C-magnet has an open access to the magnet gap which simplifies the beam pipe installation and magnetic field measurements. Coils around poles because of small bending radiuses should be wound from the rather small copper conductor. This drives the design to the large: number of turns, coil voltage, inductance, and parallel water circuits with small water cooling holes, and as a result to the individual power supply for each magnet. The variation of ampere-turns along the magnet at the constant magnet gap could be provided by magnet poles separation in the longitudinal direction but having the common return yoke as in MAX IV [4, 5]. But in this case the magnet pole will have 4 slots for coil sections ends and the magnet gap field will have the strong coupling between various magnet sections having parallel paths for the magnetic flux. Most of these variants were investigated. Some specification constraints: magnet field variations, magnet open side gap, connecting all M1 or M2 magnets in series drive the design to the variant 5. It was decided to build the M1 C-magnet prototype to confirm the design, fabrication technology, magnet performance, and magnetic measurement technique.

For the M1 magnet design the C-magnet with the single coil on the backleg of the yoke was chosen. The field gradient along Z-axis obtained by the magnet air gap variation (see Fig. 2). It has following advantages:

- C-magnet with the open gap is easily for the beam pipe installation, access, Hall probe measurements, vacuum ports mounting, and tolerance control.
- There is no coupling between 5 magnet sections as in other variants.
- The smooth magnet gap variation produces the smooth magnetic field along Z-axis with low high order field harmonics content.
- Single coil design reduces the cost of fabrication.
- Placing the coil around the yoke backleg opens the possibility of using relatively large copper conductors with high current needed when 80 magnets are connected in series. It reduces voltage to the ground to the reasonable 500 V value.

Nevertheless, it should be noted that usual C-magnet yoke is a little bit larger than H-magnet, the air gap increase should be combined with some pole width increase, pole shims in the C-magnet are non-symmetrical, for the long coil the power losses are larger, and there is an additional fringe field from the outer part of the coil. All of these could be rather easy resolved, and could not overcome advantages described above.

There should be fabricated 80 M1, and 80 M2 magnets. All magnets or groups of them could be connected in series and powered by a single power supply.

The M1 dipole magnetic design is based on the 3D magnetic field simulations by TOSCA code [6]. Initially 2D simulations were performed and pole profiles optimizations for three magnet cross-sections having peak fields: 0.634 T, 0.341 T, and 0.131 T. The specified magnetic fields were obtained by the air gap variations: 27 mm, 48 mm, and 126 mm. The pole profile in the transition area from the gap 48 mm to 126 mm was obtained by the linear transformation. Shims have rectangular form and placed at pole edges.

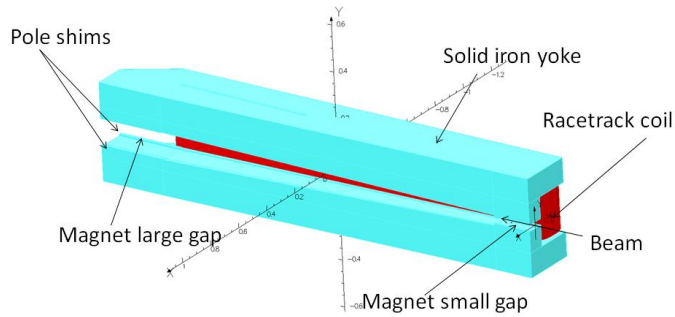

Fig. 2. The L-Bend dipole magnet geometry.

For the M2 magnet the gap variation will be less which is easier to provide. This is why for the test model the M1 was chosen because it is a more complicated magnet with larger magnetic field dBy/dz gradient, and the air gap variation. Fig. 3 shows the magnetic field distribution along Z-axis in the center line of magnet aperture.

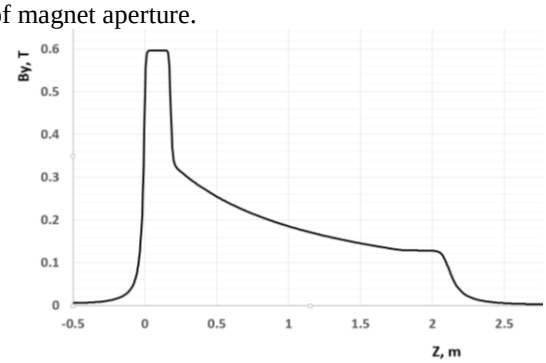

Fig. 3. Calculated magnetic field for 182 A for x = y = 0.

Fig. 4 shows the field homogeneity of the simulated 3D magnetic field. The difference in the field homogeneity caused by the linear gap, pole width and shims variations along z-axis. The electron beam is rather small but for the straight magnet the good field area including Sagitta will be ±5 mm. In this area the calculated field homogeneity is in the range of 2 units (2×10^{-4}).

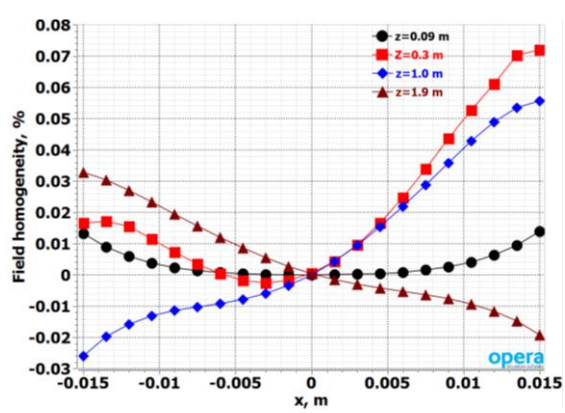

Fig. 4. Calculated magnetic field homogeneity in the vertical midplane (y=0).

The integrated magnetic field harmonics along z-axis at the reference radius 10 mm are in the range of 1 unit. The peak harmonics values along the magnet good field area are for: the quadrupole -3.5 units, sextupole 11.5 units, octupole 0.3 units, and very small for all others.

Copyright (c) 2016 IEEE. Personal use is permitted. For any other purposes, permission must be obtained from the IEEE by emailing pubs-permissions@ieee.org.

This is the author's version of an article that has been published in this journal. Changes were made to this version by the publisher prior to publication.
The final version of record is available at http://dx.doi.org/10.1109/TASC.2016.2521896

The calculated M1 magnet model parameters are shown in Table 2. The racetrack winding is wound from the hollow copper conductor around the magnet yoke backleg (see Fig. 2). The winding consists of nine double pancake coils connected in series. The conductor has glass tape insulation. The winding is vacuum impregnated by the epoxy CTD-101 and after that cured in an electrical oven. The magnet yoke is assembled from a low carbon steel AISI 1010 blocks bolted together with the coil block, and the stainless steel support plate (see Fig. 5). The magnet has parallel pole surfaces at both end blocks for the more easy dimensions and the field control. The coil is cooled by a water and has three parallel water cooling circuits. The magnet voltage and current matched to the purchased Danfysik power supply. An existing copper conductor at FNAL was chosen for the magnet prototype.

TABLE 2

M1 MAGNET PARAMETERS

Parameter	Unit	M1 Prototype	M1 Production Model
Pole length	m	2.09	2.09
Small gap	mm	26	26
Large gap	mm	126	126
Copper conductor	mm	10.4×10.4 dia. 5.8	15×15 dia. 8.5
Number of turns		72	24
Number of sections		9	4
Coil current	A	184	573
Coil resistance	mΩ	64	10.2
Coil voltage drop	V	12.2	6.0
Power loss/magnet	kW	2.3	3.5
Water pressure	MPa	0.56	0.56
Water circuits		3	1
Water temperature rise	°C	5	9

The M1 prototype magnet is designed for the relatively low 184 A current which is more robust for magnetic measurement test stands. In the final configuration there could be 80 magnets connected in series. It is desirable to make the peak voltage to the ground no more than 500 V. In this case coils will be wound even with larger conductor dimensions, and the current will be around 573 A as shown in Table 2 for the production model.

Because M2 magnet has about the same integrated field, effective length as M1, and two times lower peak field it is possible by using two M1 winding double pancakes power M2 magnet. With the small variation of the M2 first section effective length it is possible to make the M2 current the same as in M1. In this case all M1 and M2 magnets could be connected in series and powered by a single power supply. The winding power losses could be reduced by making the coil and the backleg closer to a square area, and by using a larger copper conductor. The proper choice of the conductor current density should be made based on the balance between capital and operational expenses for the whole magnet system. It should be noted that in most accelerator magnets designed for the long term operations the optimal current density is close to the 4 A/mm^2.

One of the possible drawbacks for the proposed magnet configuration are fringe fields at magnet pole ends. These fields could be reduced by ferromagnetic shields. The 126 mm magnet gap end field has comparable with 26 mm gap absolute field value at the same distance from the pole end (0.04 T at 100 mm distance from both ends). It is explained by the same relation between large and small gap, and the same relation between the large and low peak fields at both magnet pole ends.

III. MAGNETIC MEASUREMENTS

High precision magnetic field measurements were performed at both the FNAL (Fig. 5) and the ANL (Fig. 6) laboratories. The goal of the magnetic measurements was to check the magnetic design calculations and to verify that the specifications were met by comparing measured magnetic field quantities from two independent measurement stations.

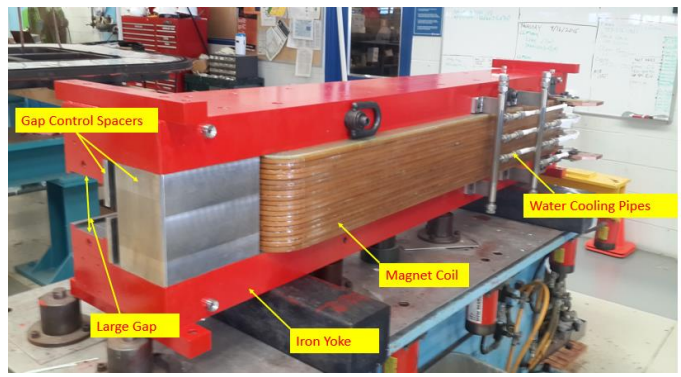

Fig. 5. The M1 longitudinal gradient dipole magnet prototype at the FNAL.

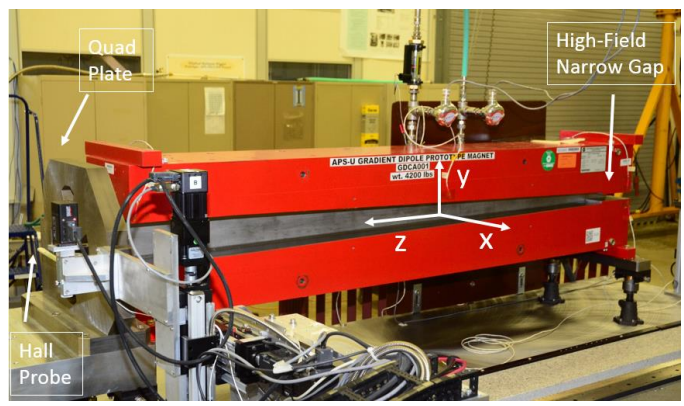

Fig. 6. The M1 magnet setup on the ANL test stand for high-precision Hall probe magnetic measurements.

The FNAL measurements were made largely with a small self-contained rotating coil device referred to as a 'Ferret' (FERmilab Rotating-coil Encapsulated Tesla-probe) [7]. The Ferret used here has a 26-mm-long printed-circuit radial coil having 14 layers with 10 loops per layer. An analog bucking circuit suppresses the dipole at a level of ~700 and allows sensitive measurement of the harmonics. The probe has a rotation diameter of 22.5 mm and is enclosed in a carbon fiber tube with OD of 25.4 mm. A miniature encoder with 512 samples/rev and slip-rings are also contained within the tube, and the probe is rotated via a flexible drive shaft with external motor on the measurement data acquisition cart. The probe was affixed to an aluminum arm and translated through the magnet

Copyright (c) 2016 IEEE. Personal use is permitted. For any other purposes, permission must be obtained from the IEEE by emailing pubs-permissions@ieee.org.

This is the author's version of an article that has been published in this journal. Changes were made to this version by the publisher prior to publication.
The final version of record is available at http://dx.doi.org/10.1109/TASC.2016.2521896

on the rails of the test stand. A linear actuator could translate the probe over about 275 mm in 25 mm steps, but manual translation was required to reposition the assembly to subsequent actuator stations to cover the full magnet length. A laser tracker target was mounted on the shell of the probe to record with some higher accuracy the position of the probe.

The ANL magnetic measurements were performed with a scanning Hall probe system, which used a two-axis (Bx, By) Senis Hall probe (model 046-12) to take data on-the-fly at a speed of 200 mm/sec recorded every 0.2 mm. The relative reproducibility of the field and the field integral measurements is better than 1.0×10^{-4} for high magnetic fields, which is the case here, and the reproducibility of the Z position is better than 2 µm [8, 9].

Figure 7 compares the measured magnetic field as a function of Z of the Ferret and Hall probe. The field homogeneity measured by both systems is presented in Fig. 8 for 177A.

These data show excellent correspondence to the calculated fields presented in Figs. 3 and 4, and demonstrate that the required field homogeneity of less than 0.02 % in the region x = ±5 mm region has been achieved.

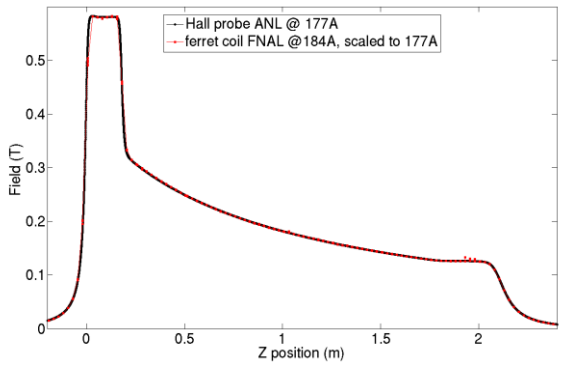

Fig. 7. Measured magnetic fields by the ANL and the FNAL.

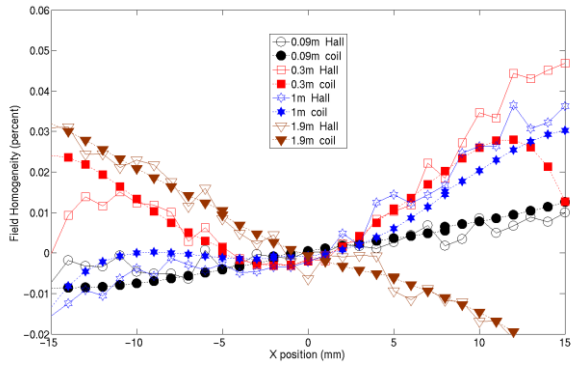

Fig. 8. Measured magnet field homogeneities at different positions along the Z-axis. The field shape for the rotating coil is reconstructed from the harmonics measured at three overlapping probe positions across the aperture.

Fig. 9 shows the measured integrated magnetic field by the ANL Hall probe compared to the results derived from the design model. The minor differences seen can be explained by differences in magnetic properties of the low carbon steel and differences in the model geometry used in the simulations compared to the as-built magnet. Fig. 10 shows a close-up view of the same measured magnetic field integrals compared to those obtained with the stretched wire system at the FNAL.

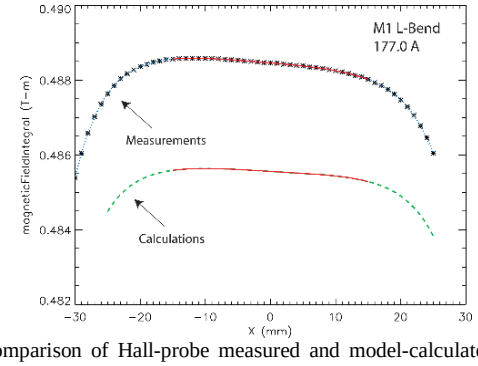

Fig. 9. Comparison of Hall-probe measured and model-calculated magnetic field integrals. Calculations were scaled to 177 A.

A range of ±15 mm was used for the fit of the multipole coefficients (see Fig. 9). The fit is shown by the red solid curve and the stars indicate the measured data points. The fitted integrated field is 0.48846 T-m (measured) and 0.48556 T-m (calculated) and the fitted quadrupole gradient is -149 G (measured) and -107 G (calculated).

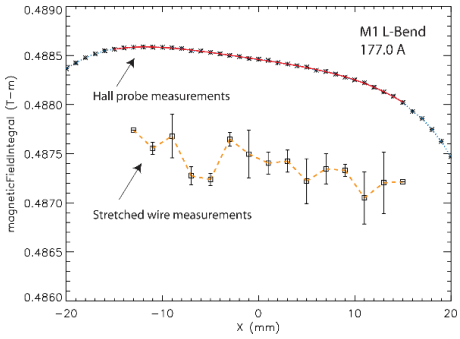

Fig. 10. Close-up view of the measured magnetic field integrals obtained with two different techniques. Stretched wire measurements were scaled to 177 A.

IV. Conclusion

A longitudinal gradient dipole was designed, built, and successfully tested and measured by the ANL-FNAL collaboration. The magnet prototype test results showed:

- A viable magnet design concept.
- Accurate magnetic field measurements at the ANL and FNAL laboratories were in good agreement.
- Good fabrication and assembly tolerances were achieved to provide excellent agreement between designed and measured magnetic fields.

All of these opens the way to proceed with the production magnets design and fabrication.

References

[1] "Advanced Photon Source", https://www1.aps.anl.gov/APS-Upgrade
[2] M. Borland, *et al*, "Hybrid Seven-Bend-Achromat Lattice for the Advanced Photon Source Upgrade," Proc. of IPAC2015, Richmond, VA, USA, TUPJE063.

Copyright (c) 2016 IEEE. Personal use is permitted. For any other purposes, permission must be obtained from the IEEE by emailing pubs-permissions@ieee.org.

This is the author's version of an article that has been published in this journal. Changes were made to this version by the publisher prior to publication.
The final version of record is available at http://dx.doi.org/10.1109/TASC.2016.2521896

[3] M. Jaski, *et al*, "Magnet Designs for the Multi-Bend Achromat Lattice at the Advanced Photon Source," Proc. of IPAC2015, Richmond, VA, USA, WEPTY003.
[4] S. C. Leemann, *et al*, "Status of the MAX IV Storage Rings," Proc. of IPAC'10, Kyoto, Japan, WEPEA058.
[5] "MAX-IV Detailed Design Report," https://www.maxlab.lu.se/sites/default/files/maxiv_ddr_2_5_MAX_IV_Magnets.pdf
[6] OPERA 3D TOSCA, Cobham Technical Services, Vector Fields Software, 24 Bankside, Kidlington, Oxford OX5 1JE, England.
[7] J. DiMarco, *et al*.,"Application of PCB and FDM Technologies to Magnetic Measurement Probe System Development", *IEEE Transactions on Applied Superconductivity,* vol. 23, no. 3, 9000505, June 2013.
[8] I. Vasserman, *et al*, "Insertion Devices: Magnetic Measurements and Tuning,"ANL/APS/TB-53, October 2010. https://www1.aps.anl.gov/Science/Publications/Technical-Bulletins
[9] I. Vasserman, *et al*, "Some aspects of achieving an ultimate accuracy during insertion device magnetic measurements by a Hall probe," Rev. Sci. Instrum. 84 (2), 025004 -1-025004 -7 (2013). DOI: 10.1063/1.4790422.

Copyright (c) 2016 IEEE. Personal use is permitted. For any other purposes, permission must be obtained from the IEEE by emailing pubs-permissions@ieee.org.